INTERNATIONAL JOURNAL FOR NUMERICAL METHODS IN FLUIDS
Int. J. Numer. Meth. Fluids 2002; **40**:583–592 (DOI: 10.1002/fld.304)

Dynamic subgrid modelling for time dependent convection–diffusion–reaction equations with fractal solutions

Johan Hoffman *

Mathematical Department, Chalmers University of Technology SE-412 96 Göteborg, Sweden

SUMMARY

A dynamic scale similarity model is proposed. The subgrid model is tested for model problems related to time dependent non-linear convection–diffusion–reaction systems with fractal solutions. The error of an approximate solution with subgrid model on a scale h is typically smaller than that of a solution without subgrid model on the scale $h/2$. We also consider the problem of *a posteriori* error estimation for fractal solutions, splitting the total computational error into a numerical error, related to the discretization of the continuous equations, and a modelling error, taking into account the quality of the subgrid model. Copyright © 2002 John Wiley & Sons, Ltd.

KEY WORDS: wavelets; dynamic subgrid modelling; *a posteriori* error estimation

INTRODUCTION

In recent years methods of *dynamic subgrid modelling* have been proposed, in particular in turbulence modelling in *Dynamic Large Eddy Simulations* (DLES) by Germano *et al.* [1]. The purpose of a subgrid model is to model the effect of unresolvable scales on resolvable scales corresponding to closure in turbulence modelling. The basic idea in dynamic subgrid modelling is to fit a particular subgrid model based on computed solutions on different resolvable scales, and then extrapolate the model to subgrid scales. In order for such a process based on scale extrapolation to work, it is necessary that the underlying problem has some 'scale regularity', so that the experience gained by fitting the model on a coarse scale with a fine scale solution as reference may be extrapolated to the finer scale. There is empirical evidence ([2, 3] and references therein) that many problems involving a range of scales from large to small, such as fluid flow at larger Reynolds numbers and flow in heterogeneous porous media, in fact do have such a regularity, once the larger scales related to the geometry of the particular problem have been resolved.

The purpose of this note is to study the feasibility of the indicated dynamic subgrid modelling procedure in the context of some model problems related to convection–diffusion–

* Correspondence to: J. Hoffman, Mathematical Department, Chalmers University of Technology, SE-412 96 Göteborg, Sweden.

Received May 2001
Revised September 2001

reaction systems with 'fractal' solutions, where the fractality originates from data. In this paper, we study time dependent problems, extending the study of stationary problems in References [4–6]. The relevance of studying fractal models is motivated by the abundant number of experimental observations of fractality in e.g. turbulent flows (see e.g. Reference [3]).

PROBLEM FORMULATION

We consider the model problem: Find $u : \Omega \times [0,T] \to \mathbb{R}^n$ such that

$$\dot{u} + Lu = \dot{u} - \varepsilon \Delta u + \beta \cdot \nabla u = f(u), \quad \forall (x,t) \in \Omega \times (0,T) \tag{1}$$

$$u = u_D, \quad \forall (x,t) \in \Gamma_D \times (0,T), \quad \frac{\partial u}{\partial n} = u_N, \quad \forall (x,t) \in \Gamma_N \times (0,T) \tag{2}$$

$$u(x,0) = u_0(x), \quad \forall x \in \Omega \tag{3}$$

where $f : \mathbb{R}^n \to \mathbb{R}^n$ is smooth, $\Omega \subset \mathbb{R}^d$ and $\partial\Omega = \Gamma_D \cup \Gamma_N$. Typically we will assume that ε is small and that the solution u to (1)–(3) contains a range of scales, from very small scales to large scales, induced by either the initial condition $u_0(x)$ or the differential operator L through β. Assuming we want to find an approximation of u on the scale h, representing the finest spatial computational scale, we define for each fixed t the spatial *running average* u^h of u on the scale h by

$$u^h(x,t) = \frac{1}{h^d} \int_{x_1-h/2}^{x_1+h/2} \cdots \int_{x_d-h/2}^{x_d+h/2} u(y,t)\, \mathrm{d}y_1 \ldots \mathrm{d}y_d \tag{4}$$

where we note that this operator commutes with space and time differentiation. Applying this operator to (1)–(3) we find that the running average u^h satisfies the equation

$$\dot{u^h} + L_h u^h = \dot{u^h} + \beta^h \cdot \nabla u^h - \varepsilon \Delta u^h = f(u^h) + F_h(u), \quad u^h(x,0) = u_0^h(x) \tag{5}$$

where L_h is a simplified operator on the scale h resulting from approximating β by β^h and the correction term $F_h(u) = (f(u))^h - f(u^h) + L_h u^h - (Lu)^h$ contains the influence of the unresolved scales on u^h. We consider a computational problem without subgrid model of the form

$$\dot{u}_h + L_h u_h = f(u_h), \quad u_h(x,0) = u_0^h(x) \tag{6}$$

and a corresponding problem with subgrid model of the form

$$\dot{\tilde{u}}_h + L_h \tilde{u}_h = f(\tilde{u}_h) + \tilde{F}_h(\tilde{u}_h), \quad \tilde{u}_h(x,0) = u_0^h(x) \tag{7}$$

where $\tilde{F}_h(\tilde{u}_h)$ should approximate $F_h(u)$. In this paper, we will consider a subgrid model of the form $\tilde{F}_h(\tilde{u}_h) = g(F_h(\tilde{u}_h), F_{2h}(\tilde{u}_h), F_{4h}(\tilde{u}_h))$, where the function g is derived based on a scale regularity assumption on $F_h(u)$.

ANALYSIS OF $F_h(u)$ USING THE HAAR MRA

In the rest of this paper, we let $\Omega = [0,1]^2$ and for each $h = 2^{-i}$, with $i = 0, 1, \ldots$, we define a corresponding regular quadratic mesh τ^h with elements corresponding to subdomains $\Omega_{i,k}$ with side length h. We denote the space of piecewise constant functions on τ^h by V_i, and the closure of the union of the V_j's is equal to $L_2(\Omega)$. The chain of closed subspaces $V_0 \subset V_1 \subset \cdots \subset V_j \subset \cdots$ is denoted a *Haar Multiresolution Analysis* (MRA) of $L_2(\Omega)$ [7]. Each V_j is spanned by the dilates and integer translates of one *scale function* $\Phi \in V_0$, that is, $V_j = \text{span}\{\Phi_{j,k}(x) = 2^j \Phi(2^j x - k)\}$. The functions $\Phi_{j,k}$ form an L_2-orthonormal basis in V_j, and we denote the orthogonal complement of V_j in V_{j+1} by W_j, which is generated by another orthonormal basis (the *wavelets*) $\Psi_{j,k}(x) = 2^j \Psi(2^j x - k)$, where $\Psi \in W_0$ is called the *mother wavelet*. $W_j = W_j^1 \oplus W_j^2 \oplus W_j^3$, where the W_j^v's represent differences in the horizontal, vertical and diagonal directions, respectively. The space $L_2(\Omega)$ can now be represented as the direct sum $L_2(\Omega) = V_0 \oplus W_0^1 \oplus \cdots \oplus W_0^3 \oplus \cdots \oplus W_j^1 \oplus \cdots \oplus W_j^3 \oplus \cdots$, and each $f \in L_2(\Omega)$ has a unique decomposition $f = f_\Phi \Phi + \sum_{j,k} f_{j,k}^1 \Psi_{j,k}^1 + \cdots + f_{j,k}^3 \Psi_{j,k}^3 = f_\Phi + \sum_j f_j^1 + \cdots + f_j^3$, where the f_j^v's represent the contributions on the different scales 2^{-j}. For the one-dimensional Haar MRA in $L_2([0,1])$, the scale function is defined by $\varphi(x) = 1$ for $x \in (0,1)$ and 0 else, and the mother wavelet is defined by $\psi(x) = 1$ for $x \in (0, \frac{1}{2})$, -1 for $x \in (\frac{1}{2}, 1)$ and 0 else. In two-dimensions the scale function and the wavelets are tensor products of the one-dimensional scale function and wavelets. For the two-dimensional Haar MRA in $L_2(\Omega)$ we have the scale function $\Phi(x_1, x_2) = \varphi(x_1)\varphi(x_2)$ and the wavelets $\Psi^1(x_1, x_2) = \varphi(x_1)\psi(x_2)$, $\Psi^2(x_1, x_2) = \psi(x_1)\varphi(x_2)$, $\Psi^3(x_1, x_2) = \psi(x_1)\psi(x_2)$.

Definition 1
For $f \in L_2(\Omega)$, we define $[f]^h = f_\varphi + \sum_{j<i} f_{j,k}^1 \Psi_{j,k}^1 + f_{j,k}^2 \Psi_{j,k}^2 + f_{j,k}^3 \Psi_{j,k}^3$.

The linear mapping $L_2 \ni f \to [f]^h \in V_i$ can then be identified with the L_2-projection of f onto V_i, and we note that $[f]^h = \bar{f}^h$, where $\bar{f}^h$ is the piecewise constant function on τ^h that equals f^h in the midpoints of each element in τ^h. If we let $\bar{F}_h(u)$ denote the piecewise constant function on τ^h that equals $F_h(u)$ in the midpoints of the elements of τ^h, we have

$$\bar{F}_h(u) = [f(u)]^h - f([u]^h) - ([\beta \cdot \nabla u]^h - [\beta]^h \cdot [\nabla u]^h)$$

which for second-order reaction terms $f(u)$ leads us to model covariances of the form

$$E_h(v, w) = [vw]^h - [v]^h [w]^h \tag{8}$$

for given functions v and w. The following lemma from Reference [5] shows that $E_h(v, w)$ equals a mean of all Haar coefficients corresponding to Haar basis functions with support in $\Omega_{i,k}$.

Lemma 1
For

$$x \in \Omega_{i,k} \Rightarrow E_h(v, w)(x) = 2^{2i} \sum_{\substack{j \geqslant i \\ l:\Omega_{j,l} \subset \Omega_{i,k}}} (v_{j,l}^1 w_{j,l}^1 + v_{j,l}^2 w_{j,l}^2 + v_{j,l}^3 w_{j,l}^3)$$

SCALE EXTRAPOLATION USING SELF-SIMILARITY

By a *fractal* or *self-similar* function we mean, in this paper, a function that has some sort of scale similarity, following one of several definitions of a fractal by Mandelbrot [8]: *A fractal is a shape made of parts similar to the whole in some way*.

In Large Eddy Simulations (LES) the objective of subgrid modelling is to model the divergence of the exact Reynolds stress tensor $\tau_{ij} = (u_i u_j)^h - u_i^h u_j^h$, where each component has the form of a covariance similar to (8). There is an agreement of the existence of an inertial range in the energy spectrum of a turbulent flow [2], and different types of scale similarity assumptions also on the Reynolds stresses have been used to motivate various subgrid models, for example in the dynamic procedure [1] the parameters in a particular model are determined by comparing different averages of the resolved Reynolds stresses. In scale similarity models [9] the assumption is that the exact Reynolds stresses are proportional to the resolved Reynolds stresses. In References [4–6] we have used an assumption based on the existence of such a scale similarity with respect to a Haar MRA generated by the hierarchy of successively refined computational meshes. This assumption is investigated in Reference [10] for a transition study of a Couette flow. The finest computational scale is $h = 2^{-6}$ and the sum of the Haar coefficients for the Reynolds stress tensor component τ_{11} are plotted for three different scales in Figure 1. Component τ_{11} is chosen since the streamwise velocity dominates the Couette flow. The transition to turbulence has started even though it is not fully developed, and the plot shows 60 elements in the coarsest mesh corresponding to the scale $8h$, and we see that the decrease in the Haar coefficients is reasonable regular and we consider this as some evidence of scale similarity of the Reynolds stresses for this flow, in the form of a power law for the sum of Haar coefficients on each scale. Scale similarity with respect to a Haar MRA has also been observed in experimental aerothermal data [11]. We will base our subgrid model on an Ansatz of the form

$$E_h(v,w)(x) = C(x)h^{\mu(x)}, \quad x \in \Omega \tag{9}$$

The Ansatz (9) can be derived using Lemma 1 for the special case when the Haar coefficients of the functions v and w in (8) have the form $v_{j,k}^v = \alpha_v(x)2^{-j(1+\delta_v(x))}$ and $w_{j,k}^v = \beta_v(x)2^{-j(1+\gamma_v(x))}$, respectively, which corresponds to the simple self-similar forms $v_{j+1} = 2^{-\delta(x)}v_j$ and $w_{j+1} = 2^{-\gamma(x)}w_j$. We then have, assuming $\alpha_v, \beta_v, \delta_v, \gamma_v \in V_i$, that $E_h(v,w)(x) = C_1(x)h^{\mu_1(x)} + C_2(x)h^{\mu_2(x)} + C_3(x)h^{\mu_3(x)}$, where $C_v = \alpha_v\beta_v/(1-2^{-\mu_v})$ and $\mu_v = \delta_v + \gamma_v$. The proof is in Reference [5], and for the case when $\delta_1 = \delta_2 = \delta_3$ and $\gamma_1 = \gamma_2 = \gamma_3$ we get (9). Lemma 1 further gives:

Proposition 2

$$E_{2^k h}([v]^h, [w]^h) = E_{2^k h}(v,w) - E_h(v,w), \quad 0 \leqslant k \leqslant i$$

Proof
By Lemma 1, $E_{2^k h}(v,w)$ is a sum over the scales $j \geqslant i-k$. Split this sum into two sums: one sum over the scales $j \geqslant i$ which is equal to $E_h(v,w)$, and one sum over the scales $i-k \leqslant j < i$ which is equal to $E_{2^k h}([v]^h, [w]^h)$. □

In the following, we let $E_h(x)$ mean $E_h(v,w)(x)$ if nothing else is stated, and we now use the Ansatz (9) to derive the following propositions:

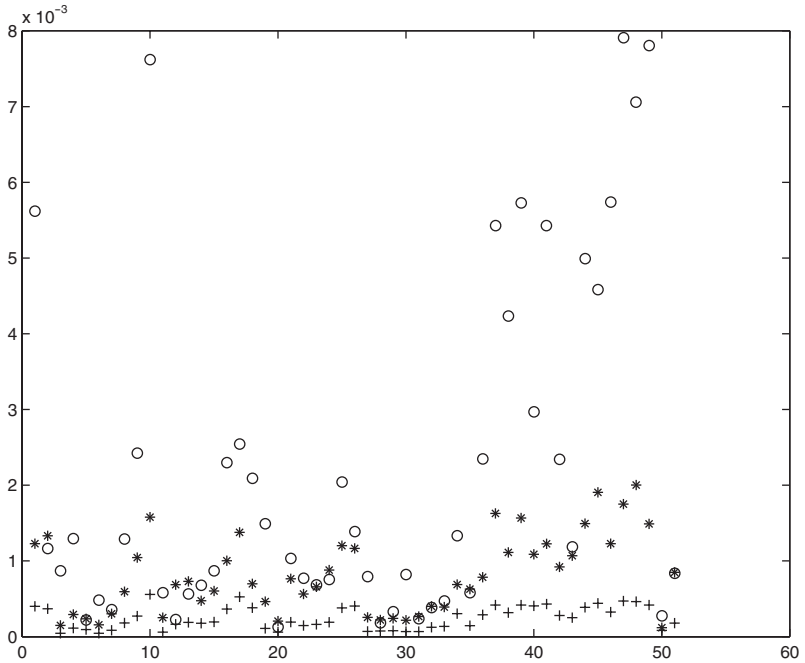

Figure 1. Sum of Haar coefficients for $\tau_{11}^{8h}(U_h)$ on scales $8h$ ('o'), $4h$ ('$*$'), and $2h$ ('$+$').

Proposition 3
Assume that (9) is valid with C, $\mu \in V_{i-2}$, then

$$E_h(v,w) = (E_{2h}(v,w) - E_h(v,w)) \Big/ \left(\frac{E_{4h}(v,w) - E_{2h}(v,w)}{E_{2h}(v,w) - E_h(v,w)} - 1 \right)$$

Proof
Using that $E_h, E_{2h} \in V_{i-2}$, (9) gives that

$$\frac{E_{4h} - E_{2h}}{E_{2h} - E_h} = \frac{C(4h)^\mu - C(2h)^\mu}{C(2h)^\mu - Ch^\mu} = 2^\mu$$

and in the same way we have that $E_{2h} - E_h = Ch^\mu(2^\mu - 1) = E_h(2^\mu - 1) \Rightarrow E_h = (E_{2h} - E_h)/(2^\mu - 1)$ □

Proposition 4
Assume that (9) is valid with C, $\mu \in V_{i-2}$, then

$$E_h([v]^{2^{-n}h}, [w]^{2^{-n}h})(v,w) = \left(1 - \left(\frac{E_{4h}(v,w) - E_{2h}(v,w)}{E_{2h}(v,w) - E_h(v,w)} \right)^{-n} \right) E_h(v,w)$$

Proof
Proposition 2 $\Rightarrow E_h([v]^{2^{-n}h},[w]^{2^{-n}h}) = E_h(v,w) - E_{2^{-n}h}(v,w) = Ch^\mu(1-2^{-n\mu}) = E_h(v,w)(1-2^{-n\mu})$, and we finally have 2^μ from the proof of Proposition 3. □

Propositions 2–4 motivates, for each t, an approximation of $[E_h(v,w)]^{4h}$, since an underlying assumption in Propositions 3 and 4 was that $E_h(v,w) \in V_{i-2}$. Each component of $\bar{F}_h(u)$ is a sum of terms of the form (8) and we use Propositions 3 and 4 to approximate each of these terms. We can use Proposition 2 to express these approximations in terms of $[v]^h$, $[w]^h$ instead of v, w, which is desirable since we will only have access to approximative solutions $\tilde{v}_h$, $\tilde{w}_h$on the scale h. If $\tilde{\bar{F}}_h(\tilde{u})_k$ denotes the approximation of $\bar{F}_h(u)_k$, the kth component of $\bar{F}_h(u)$, and $2^{-n}h$ is the finest scale in the exact solution u, we have a subgrid model of the form

$$\bar{F}_h(u)_k = \sum E_h(v,w) \quad \Rightarrow \quad \tilde{\bar{F}}_h(\tilde{u}_h)_k = \sum \tilde{E}_h(\tilde{v}_h,\tilde{w}_h) \tag{10}$$

$$\tilde{E}_h(\tilde{v}_h,\tilde{w}_h) = \left(1 - \left(\frac{E_{4h}(\tilde{v}_h,\tilde{w}_h) - [E_{2h}(\tilde{v}_h,\tilde{w}_h)]^{4h}}{[E_{2h}(\tilde{v}_h,\tilde{w}_h)]^{4h} - [E_h(\tilde{v}_h,\tilde{w}_h)]^{4h}}\right)^{-n}\right) \times \frac{[E_{2h}(\tilde{v}_h,\tilde{w}_h)]^{4h} - [E_h(\tilde{v}_h,\tilde{w}_h)]^{4h}}{\dfrac{E_{4h}(\tilde{v}_h,\tilde{w}_h) - [E_{2h}(\tilde{v}_h,\tilde{w}_h)]^{4h}}{[E_{2h}(\tilde{v}_h,\tilde{w}_h)]^{4h} - [E_h(\tilde{v}_h,\tilde{w}_h)]^{4h}} - 1}$$

A POSTERIORI ERROR ANALYSIS

A general strategy for *a posteriori* error analysis based on duality is described in Reference [12]. In this section we will make some remarks concerning the non-linear problems with fractal solutions that appear in this paper. We assume that u is the solution to (1)–(3) and that U is a numerical approximation to the solution of either (6) or (7). The standard technique to obtain *a posteriori* error estimates for the error $e = u - U$ is a chosen norm to introduce a linearized dual problem of the form: $-\dot{\varphi} - A(u,U)^*\varphi = 0$, $\varphi(T) = \varphi_T$, where $*$ denotes the transpose. The choice of φ_T determines in what norm we estimate e, for example, $\varphi_T = e(T)/\|e(T)\|$ gives a L_2-estimate of e. Here $\|\cdot\|$ denotes the L_2-norm and we further let $(\cdot,\cdot)$ denote the L_2-inner product. Following Reference [12] (assuming continuous approximation in time) we get for $\varphi_T = e(T)/\|e(T)\|$ that

$$\|e(T)\| = (e(T), e(T)/\|e(T)\|) = (e(T),\varphi(T)) + \int_0^T (e, -\dot{\varphi} - A(u,U)^*\varphi)\,\mathrm{d}t$$

$$= (e(0),\varphi(0)) + \int_0^T (\dot{e} + A(u,U)e, \varphi)\,\mathrm{d}t$$

Now if we choose $A(u,U)$ such that $A(u,U)e = Lu - f(u) - (LU - f(U))$ we get that

$$\|e(T)\| = (e(0),\varphi(0)) + \int_0^T (f(U) - \dot{U} - LU, \varphi)\,\mathrm{d}t$$

If $U = U_h$ is a numerical approximation of (6) we cannot expect the residual $f(U) - \dot{U} - LU$ to be small since (6) involves the simplified operator L_h and not L. If we on the other hand linearize at u^h instead of u and β^h instead of β, that is, we let $A(u, U)e = L_h u^h - f(u^h) - (L_h U - f(U))$. We then get $e(0) = 0$ (by a suitable choice of $U_h(0)$) and by (5) we get that

$$\|(u^h - U_h)(T)\| = \int_0^T (f(U_h) - \dot{U}_h - L_h U_h, \varphi)\,\mathrm{d}t + \int_0^T (F_h(u), \varphi)\,\mathrm{d}t \tag{11}$$

where we now have a numerical residual, $R(U_h) = f(U_h) - \dot{U}_h - L_h U_h$, corresponding to the discretization error in approximating (6), and $F_h(u)$ which corresponds to a modelling residual, independent of U_h. If we on the other hand let $U = \tilde{U}_h$ be a numerical approximation of (7), we get that

$$\|(u^h - \tilde{U}_h)(T)\| = \int_0^T (\tilde{F}_h(\tilde{U}_h) + f(\tilde{U}_h) - \dot{\tilde{U}}_h - L_h \tilde{U}_h, \varphi)\,\mathrm{d}t + \int_0^T (F_h(u) - \tilde{F}_h(\tilde{U}_h), \varphi)\,\mathrm{d}t$$

where we now have a numerical residual, $R(\tilde{U}_h) = \tilde{F}_h(\tilde{U}_h) + f(\tilde{U}_h) - \dot{\tilde{U}}_h - L_h \tilde{U}_h$, corresponding to the discretization error in approximating (7). The second term contains the difference $F_h(u) - \tilde{F}_h(\tilde{U}_h)$, which corresponds to a modelling residual one seeks to minimize by subgrid modelling.

We conclude that if u contains unresolvable subgrid scales, then the error with respect to u^h is the appropriate error to study, and thus the dual problem to be solved should be linearized at u^h and not at u. The dual problem then does not contain any scales finer than h, which means that it will be easy to solve and in particular no subgrid modelling is needed. This linearization also naturally splits the *a posteriori* error estimates in two terms, one involving a numerical residual and one involving a modelling residual, which enables us to balance the errors from discretization and subgrid modelling. In estimating the error $u^h - U_h$ by (11), $F_h(u)$ is unavailable but can be approximated by the subgrid model $\tilde{F}_h(U_h)$. To estimate the difference $F_h(u) - \tilde{F}_h(\tilde{U}_h)$ further extrapolation seems to be needed.

APPLICATIONS

We will now test the model (10) for some simple model problems in two space dimensions, where the scale similarity is introduced through data. We construct two-dimensional fractal data as sums of local tensor products of the one-dimensional fractal *Weierstrass function* $W_{\gamma,\delta}(x) = \gamma \sum_{j=0}^{N} 2^{-j\delta} \sin(2^j \cdot 2\pi x)$, where we let $\gamma = \delta = 0.1$ in all examples. The motivation for the test problems is that they contain important features of reactive flow problems. The first test problem is a reaction–diffusion problem with a Volterra–Lotka type reaction term where the scale similarity appears in the initial data, simulating for example a reactor with two reacting species. We then add a small convection corresponding to a stirred reactor. The second test problem is a convection–diffusion problem where the scale similarity appears as the convecting velocity field, simulating a passive scalar in a turbulent velocity field. In all examples we will have $h = 2^{-5}$.

Table I. Error in u_1 in L_1-norm for VL with $\beta = 0$.

Subgrid model	$t = 0.5$	$t = 1.0$	$t = 1.5$	$t = 2.0$
No model	1.9×10^{-3}	7.2×10^{-3}	1.1×10^{-2}	1.1×10^{-2}
No model on $h/2$	1.4×10^{-3}	4.6×10^{-3}	7.0×10^{-3}	6.8×10^{-3}
$\tilde{F}_h(\tilde{u}_h) = F_{2h}(\tilde{u}_h, \tilde{u}_h)$	1.4×10^{-3}	4.8×10^{-3}	6.5×10^{-3}	6.3×10^{-3}
Model (10)	1.0×10^{-3}	2.8×10^{-3}	3.8×10^{-3}	4.2×10^{-3}

Table II. Error in $u_2$in L_1-norm for VL with $\beta = 0$.

Subgrid model	$t = 0.5$	$t = 1.0$	$t = 1.5$	$t = 2.0$
No model	1.4×10^{-4}	3.4×10^{-4}	2.0×10^{-4}	4.4×10^{-4}
No model on $h/2$	1.0×10^{-4}	2.1×10^{-4}	1.2×10^{-4}	2.9×10^{-4}
$\tilde{F}_h(\tilde{u}_h) = F_{2h}(\tilde{u}_h, \tilde{u}_h)$	9.0×10^{-5}	2.0×10^{-4}	1.5×10^{-4}	2.8×10^{-4}
Model (10)	7.0×10^{-5}	1.4×10^{-4}	1.5×10^{-4}	2.4×10^{-4}

Table III. Error in u_1 in L_1-norm for VL with $\beta \neq 0$.

Subgrid model	$t = 0.5$	$t = 1.0$	$t = 1.5$	$t = 2.0$
No model	2.5×10^{-5}	1.5×10^{-4}	3.4×10^{-4}	6.4×10^{-4}
No model on $h/2$	2.5×10^{-5}	1.1×10^{-4}	1.9×10^{-4}	3.3×10^{-4}
$\tilde{F}_h(\tilde{u}_h) = F_{2h}(\tilde{u}_h, \tilde{u}_h)$	2.5×10^{-5}	1.1×10^{-4}	2.1×10^{-4}	5.0×10^{-4}
Model (10)	2.0×10^{-5}	6.0×10^{-5}	2.0×10^{-4}	5.6×10^{-4}

Volterra–Lotka (VL)

We consider a reaction dominated problem of the form

$$\dot{u_1} - \varepsilon \Delta u_1 = u_1(1 - u_2), \quad \dot{u_2} - \varepsilon \Delta u_2 + \beta \cdot \nabla u_2 = u_2(u_1 - 1)$$
$$\left.\frac{\partial u}{\partial n}\right|_{\partial\Omega} = 0, \quad u(x, 0) = (W_{\gamma,\delta}^{2D}(x), 1)$$

where $\varepsilon = 10^{-6}$, which corresponds to the classical Volterra–Lotka system with small diffusion and convection in one component. We have $F_h(u) = (-(u_1 u_2)^h + u_1^h u_2^h, (u_1 u_2)^h - u_1^h u_2^h)$, and by (10) we have that $\tilde{F}_h(\tilde{u}_h) = (-\tilde{E}_h(\tilde{u}_1, \tilde{u}_2), \tilde{E}_h(\tilde{u}_1, \tilde{u}_2))$, with $n = 4$ (reference scale minus computational scale). For these problems we use a central difference-Crank–Nicolson scheme for the midpoints of the elements, where we regard these midpoint values to represent a piecewise constant approximation over the elements, and the reference scale is 2^{-9} in the computation of the error. The solutions are oscillating and both u_1 and u_2 are fractal for $t > 0$, even though $u_2(x, 0) = 1$. We want to approximate u^h, and the errors $\|u^h - U\|$ are shown in Tables I–III, where U is the error without model, without model but computed on the finer scale $h/2$ and then projected onto the scale h, with the model (10), and with the model $\tilde{F}_h(\tilde{u}_h) = F_{2h}(\tilde{u}_h, \tilde{u}_h)$ corresponding to $n = 1$, meaning that we assume that no finer scales than

Table IV. Error in L_1-norm for FC.

Subgrid model	$t=0.25$	$t=0.5$	$t=0.75$	$t=1.0$
No model	7.2×10^{-3}	1.2×10^{-2}	1.1×10^{-2}	1.1×10^{-2}
Model (10)	5.8×10^{-3}	7.2×10^{-3}	6.2×10^{-3}	6.2×10^{-3}

$h/2$ are present in the exact solution u. We first let $\beta=0$ and compute to $T=2$, then we let β be a rotational mixing of order h: $\beta=h\ (\sin(\pi x_1)\cos(\pi x_2), -\cos(\pi x_1)\sin(\pi x_2))$ and here we only compute to $T=1$, since after $T=1$ the subgrid scales are dominated by the convective streaks due to β. We study the error for each component individually, and for $\beta=0$ we find that the solution with the subgrid model (10) is the best for both components, even though the modelling errors are smaller in u_2 since $u_2(x,0)$ is constant. We also note that the solution with the subgrid model corresponding to $n=1$ is very close to the solution on the scale $h/2$ without subgrid model as expected. For $\beta\neq0$ the solution with subgrid model (10) is best for u_1 but, because of the convection, subgrid scales in u_2 do not develop and the solutions with subgrid models does not differ significantly from the solution without subgrid model. The solution on $h/2$ is better since the numerical error is then reduced.

Fractal convection (FC)

We also consider a convection dominated problem of the form

$$\dot{u}+\beta\cdot\nabla u-\varepsilon\Delta u=1,\quad u|_{x_1=0,x_2=0}=0,\quad \frac{\partial u}{\partial n}|_{x_1=1,x_2=1}=0,\quad u(x,0)=0 \tag{12}$$

for $\beta=(W^{2D}_{\gamma,\delta},W^{2D}_{\gamma,\delta})$ and $\varepsilon=10^{-3}$, which we solve by a Streamline Diffusion cG(1)cG(1) method [13] with bilinear elements. In the computation of the error the reference scale is 2^{-8}. The solution is in this case relatively smooth since the fractal β is only acting on the derivatives of the solution. We have $F_h(u)=\beta^h\cdot(\nabla u)^h-(\beta\cdot\nabla u)^h$, and in Table IV we see that the error in the solution with the subgrid model (10) is less than in the solution without subgrid model.

CONCLUSIONS

A dynamic scale similarity model for convection–diffusion-reaction problems with fractal solutions was proposed, based on a scale regularity Ansatz with respect to a Haar MRA generated by the hierarchy of successively refined computational meshes. In computational experiments the solution to a problem on the scale h with subgrid model was better than the solution to a problem on scale $h/2$ without subgrid model. We also considered the problem of *a posteriori* error estimation for these problems. We found that by linearize the dual problem at u^h, and not at u, the error representation naturally split into separate terms involving a numerical residual and a modelling residual, respectively, which enables us to balance errors from discretization and subgrid modelling.

ACKNOWLEDGEMENTS

The author would like to thank Professor Claes Johnson for his suggestions and continuous encouragement during this work.

REFERENCES

1. Germano M, Poimelli U, Moin P, Cabot W. A dynamic subgrid scale eddy-viscosity model. *Physics of Fluids A* 1991; **3**:1760.
2. Gatski TB, Hussaini MY, Lumley JL. *Simulation and Modeling of Turbulent Flow*. Oxford University Press: Oxford, 1996.
3. Scotti A, Meneveau C. Fractal dimension of velocity signal in high-Reynolds-number hydrodynamic turbulence. *Physical Review E* 1995; **51**:5594.
4. Hoffman J, Johnson C, Bertoluzza S. Dynamic Subgrid Modeling I. *Preprint. Chalmers Finite Element Center*, 2000. http://www.phi.chalmers.se/preprints/abstracts/preprint-2000-04a.html.
5. Hoffman J. Dynamic Subgrid Modeling II. *Preprint. Chalmers Finite Element Center*, 2000. http://www.phi.chalmers.se/preprints/abstracts/preprint-2000-04b.html.
6. Hoffman J. Dynamic Subgrid Modeling for Convection–Diffusion Equations with Fractal Coefficients. *Multiscale and Multiresolution Methods*: *Theory and Applications*, Lecture Notes in Computational Science, and Engineering, vol. 20. Springer: Heidelberg, 2001.
7. Daubechies I. *Ten Lectures on Wavelets*. Society for Industrial and Applied Mathematics: Philadelphia, Pennsylvania, U.S.A., 1992.
8. Mandelbrot BB. Self-affine fractal sets. In *Fractals in Physics*, Pietronero L, Tosatti E. (eds). North-Holland: Amsterdam, 1986.
9. Sarghini F, Piomelli U, Balaras E. Scale-similar models for large-eddy simulations. *Physics of Fluids* 1999; **11**:1596.
10. Hoffman J, Johnson C. Adaptive finite element methods for incompressible fluid flow. *2001 NATO-RTO Lecture Series*, Springer Lecture Series. Springer: Berlin, 2002.
11. Papanicolau G, Solna K. Wavelet based estimation of local Kolmogorov turbulence. *Long-range Dependence Theory and Applications*. Birkhauser: Basel, 2001.
12. Eriksson K, Estep D, Hansbo P, Johnson C. Introduction to adaptive methods for differential equations. *Acta Numerica* 1995; 105–158.
13. Eriksson K, Estep D, Hansbo P, Johnson C. *Computational Differential Equations*. Studentlitteratur: Lund, Sweden, 1996.

